Polarization memory of multiply scattered light

F. C. MacKintosh

Physics Department, Princeton University, Princeton, New Jersey 08544
and Exxon Research and Engineering, Annandale, New Jersey 08801

J. X. Zhu

Exxon Research and Engineering, Annandale, New Jersey 08801

D. J. Pine

Department of Physics, Haverford College, Haverford, Pennsylvania 19041

D. A. Weitz

Exxon Research and Engineering, Annandale, New Jersey 08801
(Received 5 September 1989)

Light backscattered from an optically dense random medium is shown to exhibit a pronounced polarization dependence. An unexpected memory of the incident circular polarization of multiply scattered light arises because the wave's helicity is randomized less rapidly than is its direction. A simple model is developed to account for the observed polarization dependence of the intensity and temporal correlations of the intensity fluctuations of backscattered light.

The propagation of light in optically dense random media is characterized by multiple scattering which randomizes the direction, phase, and polarization of the incident wave. This randomization accounts for the remarkable success of scalar diffusion theory in describing the transport properties of multiply scattered light.[1−5] Recent experiments[6,7] have demonstrated the power of this approach by extending traditional quasielastic light scattering to the multiple scattering regime, thereby allowing one to probe the structure and dynamics of optically dense media. The diffusion approximation, however, fails to fully describe *backscattered* light, because such light is comprised of a significant contribution of *multiply scattered modes* whose path lengths are comparable to the transport mean free path.[8] In this Rapid Communication, we demonstrate that these modes lead to a remarkable and unexpected persistence of polarization of multiply scattered light. Single Rayleigh scattering is known to result in the polarization of scattered light in a cloudless blue sky. What is surprising is that for *circularly* polarized light, randomization of the polarization requires many more scattering events than are required for the complete randomization of the wave's direction. This polarization memory has important consequences both for the average scattered intensity and for the temporal correlation of the intensity fluctuations of light backscattered from a time varying medium. In particular, we show that contrary to previous reports,[9] the form of the autocorrelation functions is not universal, but instead depends on both particle size and polarization.

To demonstrate the polarization memory in a multiply scattering medium, we consider a system composed of uncorrelated and noninteracting spherical particles of radius a, suspended in a liquid. The multiply scattered light results in a random speckle pattern, which fluctuates as the particles undergo Brownian motion. The backscattered intensity is comprised of the contributions of light following many different scattering paths. Each path leads to a decay of the temporal correlations of the scattered field, which depends on the number of scattering events, and consequently the path length. The field autocorrelation function is[6,7]

$$G_1(t) \equiv \langle E(t)E^*(0) \rangle \propto \int P(s)e^{-2(t/\tau_0)s/l^*}ds .$$

Here, $P(s)$ is the number of scattering paths of length s and $\tau_0 = (\lambda/2\pi)^2/D_S$, where λ is the optical wavelength in the liquid and D_S is the self-diffusion coefficient of the suspended particles. The time averaged intensity is given by $G_1(0)$. The transport mean free path l^* signifies the distance the light must travel before its direction becomes completely randomized. For $s > l^*$, $P(s)$ can be calculated within the diffusion approximation. For shorter paths, however, the diffusion approximation fails to characterize $P(s)$. Backscattered light involves many photon paths which penetrate only l^* into the medium. We focus on two limits, where a simple physical picture of the polarization dependence can be obtained. In the first case, $a \ll \lambda$, so that $l = l^*$, where l is the scattering length. Here, the nondiffusive paths involve a very small number of scattering events, and the polarization dependence reflects the behavior of single scattering at large angles. In the second case, $a \gtrsim \lambda$, and the scattering is highly anisotropic, so that $l^* \gg l$. Here, the nondiffusive paths involve many scattering events, and the polarization memory results from a slower randomization of circular polarization than of direction of propagation.

For our measurements with isotropic scatterers, with $l^* = l$, we use a 1-cm-thick sample of 0.091-μm-diam polystyrene latex spheres in water with volume concentration $\phi = 0.05$. A linearly or circularly polarized beam from a 488-nm Ar$^+$ laser is expanded to 1-cm diam and is

incident on one side of the sample. Scattered light of the desired polarization is collected from the same side of the sample. We measure the time averaged intensity $\langle I \rangle$ and the normalized intensity autocorrelation function $G_2(t)$ $\equiv \langle I(t)I(0)\rangle/\langle I\rangle^2 - 1 \propto |G_1(t)|^2$, up to a constant determined by the optics. The autocorrelation functions can be approximated by[7]

$$G_2(t) \propto e^{-2\gamma(6t/\tau_0)^{1/2}}, \tag{1}$$

where τ_0 is determined from the Stokes-Einstein relation for the self-diffusion coefficient: $D_S = k_B T(1-1.8\phi)/(6\pi\eta a)$. Here, η is the fluid viscosity, and we have corrected for the effects of hydrodynamic interactions.[10] The *slope* of the decay is characterized by the parameter γ, which directly reflects the fraction of nondiffusive paths contributing to $P(s)$, since short paths yield a slower decay of the correlations. The autocorrelation functions for the four polarization channels are plotted logarithmically versus $(t/\tau_0)^{1/2}$ in Fig. 1. All four channels exhibit nearly linear behavior in this plot, consistent with Eq. (1). However, the slopes γ depend strongly on polarization. The two linear polarization channels exhibit the largest difference in slopes, with $\gamma_{\parallel} = 1.45$ for incident and scattered light of the same polarization, while $\gamma_{\perp} = 3.06$ for light backscattered with perpendicular polarization. This difference is due to the fact that low-order backscattering sequences favor the parallel polarization channel, resulting in a smaller decay rate in this channel. The difference between the circular channels is also pronounced, with $\gamma_+ = 2.68$ for incident and scattered light of the same helicity, and $\gamma_- = 1.59$ for the opposite helicity. For circularly polarized light, low-order sequences yield backscattered light primarily of the opposite *helicity*, for which incident and reflected photons are related by mirror symmetry. The greater contribution of short paths in the parallel and opposite-helicity channels is also directly reflected in the

measured *intensity* of scattered light in these channels with $\langle I_{\parallel}\rangle/\langle I_{\perp}\rangle = 1.78$ and $\langle I_-\rangle/\langle I_+\rangle = 1.45$. In all cases the overall experimental error is about $\pm 5\%$.

The values of γ in the four polarization channels can be calculated theoretically within the *white-noise* model,[11] assuming uncorrelated particles, and $l^* = l$. The autocorrelation functions for the multiply scattered scalar[11] or vector[8] waves may be obtained from the sum of ladder diagrams, comprising the leading perturbative contribution for $l \gg \lambda$. The inclusion of the nondiffusive modes[4,8] associated with the vector model leads to the same trends in the calculated as in the measured *initial* decay of correlations: we obtain $\gamma_{\perp} = 2.7$, $\gamma_{\parallel} = 1.6$ for the linear polarization channels, and $\gamma_+ = 2.4$, $\gamma_- = 1.7$ for the circular polarization channels.

The effects of polarization on backscattering are markedly different when $a \gtrsim \lambda$. This is illustrated in Fig. 2, which shows the measured autocorrelation functions for light backscattered from 0.605-μm-diam spheres, with $\phi = 0.02$. Here, $l^* \simeq 10l$, and the two linear polarization channels have almost identical slopes: $\gamma_{\perp} = 2.18$ and $\gamma_{\parallel} = 1.96$. In addition, the average intensities in the two linear channels are almost identical, with $\langle I_{\parallel}\rangle/\langle I_{\perp}\rangle = 1.05$. *By contrast, the circular polarization channels exhibit a high degree of polarization memory.* Their relative behavior, however, has reversed: the helicity-preserving channel decays more slowly than the opposite-helicity channel. Furthermore, the helicity-preserving channel exhibits more noticeable curvature. Thus we use the initial slope to obtain $\gamma_+ = 1.72$ and $\gamma_- = 2.62$. This change is also reflected in the intensity, with $\langle I_+\rangle/\langle I_-\rangle = 1.40$.

The key to understanding these polarization effects is the behavior of paths with $s \sim l^*$. For $a \gtrsim \lambda$, the scattering from individual particles is confined to a narrow cone of angular width λ/a about the incident direction. For multiple scattering, we may regard the intermediate unit
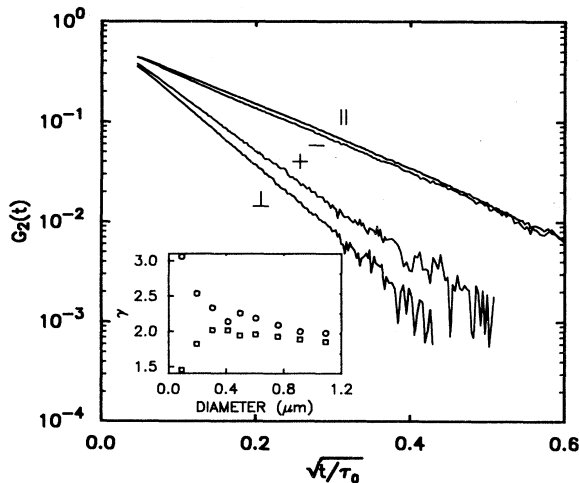

FIG. 1. Autocorrelation functions obtained for backscattering from 0.091-μm-diam polystyrene spheres for various polarization channels. Inset shows measured initial slopes γ for the linear polarization channels as a function of particle size: $\gamma_{\parallel}$ ($\square$); $\gamma_{\perp}$ ($\bigcirc$).
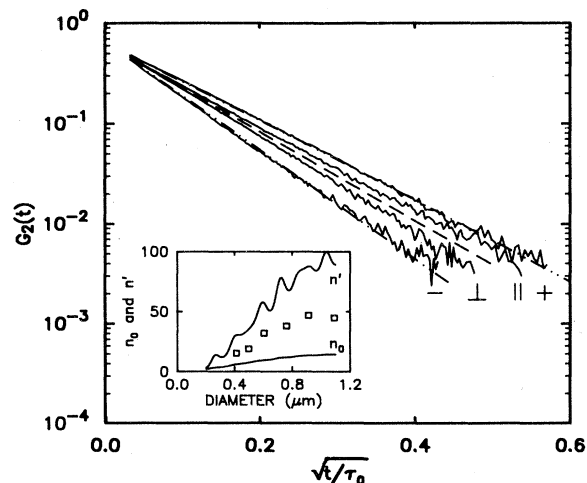

FIG. 2. Autocorrelation functions for 0.605-μm-diam spheres for various polarization channels. Autocorrelation function for unpolarized light (dashed line). Theoretical curves $G_2^{\pm}(t)$ obtained from Eq. (2) (dashed-dotted line). Inset shows calculated values of n' and n_0 vs particle size. Values of n' obtained from fits of autocorrelation functions to Eq. (2) ($\square$).

wave vectors $\hat{k}_j$ as executing a random walk on the unit sphere between incident and final directions, with small step size λ/a. The number of scattering events required to completely randomize the wave direction, $n_0 \sim (a/\lambda)^2$, provides the definition of the transport mean free path: $l^* = n_0 l$. Backscattered light is comprised of a large contribution from paths of length $s \sim l^*$, which characteristically involve n_0 scattering events. For a sufficiently large n_0, the polarization vector for incident linearly polarized light is completely randomized. A simple geometric argument demonstrates this. For each scattering event, the polarization vector $\hat{\varepsilon}_j$ is related to the previous vector $\hat{\varepsilon}_{j-1}$ by $\hat{\varepsilon}_j \propto \hat{\varepsilon}_{j-1} - (\hat{k}_j \cdot \hat{\varepsilon}_{j-1})\hat{k}_j$. In the limit of small scattering angles θ_j, this is equivalent to parallel transport of the polarization vector on the surface of the unit sphere from $\hat{k}_{j-1}$ to $\hat{k}_j$, along a great circle. Backscattering corresponds to a random walk from one pole of the unit sphere to the other. If such a path results in a backscattered wave of parallel polarization, then an equally probable path, determined by the azimuthal rotation of the sphere through an angle $\varphi = 45°$ about the incident direction, results in a backscattered wave of perpendicular polarization.[8] This reflects the azimuthal dependence of the linear polarized scattering amplitudes. Thus, paths of length $s \gtrsim l^*$ contribute equally to each linear polarization channel for large particles.

This is not the case for the circular polarization channels. For scattering through a small angle the amplitude for helicity flip is small, *independent of azimuthal rotations*. Physically, we can understand this by considering small particles. The Born approximation yields scattering amplitudes proportional to the overlap of the outgoing circular states $|R'\rangle$, $|L'\rangle$ with the incident states $|R\rangle$, $|L\rangle$:

$$\langle R' | R \rangle \propto \frac{1+\cos\theta}{2} \simeq 1$$

and

$$\langle L' | R \rangle \propto \frac{1-\cos\theta}{2} \simeq 0 .$$

For large particles, the probabilities for scattering with and without a helicity flip, $I^-(\theta)$ and $I^+(\theta)$, respectively, may be calculated within Mie theory.[12] The results are qualitatively the same as for small scatterers; for small θ, the probability of helicity flip is quite small. We may represent the *angular* average of the probabilities for scattering without $(+)$ and with $(-)$ helicity flip by

$$p_\pm = \langle I^\pm \rangle / \langle I^+ + I^- \rangle \equiv \tfrac{1}{2}(1 \pm e^{-1/n'}) .$$

Physically, $n'l$ represents the path length over which the helicity is randomized. The small amplitude for helicity flip makes this length greater than l^*. This is the origin of the polarization memory.

Paths of length $s = nl$ contributing to the two helicity channels are characterized by an even or odd number of helicity flips, respectively, each with probability p_-. The number of these paths is then given by

$$P^\pm(s) = \tfrac{1}{2}P(s)[(p_+ + p_-)^n \pm (p_+ - p_-)^n]$$

$$= \tfrac{1}{2}P(s)(1 \pm e^{-n/n'}) ,$$

where $P(s)$ is the number of scattering paths for scalar

waves. This leads to a simple expression for the autocorrelation functions in the two helicity channels in terms of the autocorrelation function for scalar waves:

$$G_1^\pm(t) \propto G_1(t) \pm G_1(t + \tau_0 n_0/(2n')) . \tag{2}$$

The second term represents a shift in the time variable, and is equivalent to the correlation function in an absorbing medium, with absorption length $n'l$. We can use Eq. (2) to compare with experiment by taking the scalar value of $\gamma = 2.05$, obtained from the unpolarized autocorrelation function, and adjusting n' to simultaneously fit both circular polarization channels. The results for 0.605-μm spheres, with $n' = 32$, are shown by the dashed lines in Fig. 2. The shapes of the autocorrelation functions are reproduced quite well, including the curvature in the helicity-preserving channel.

Physically, the polarization memory arises because n' increases with particle size more rapidly than n_0, so that more scattering events are required to randomize the helicity than to randomize the direction. The dependence on the scattering particle size is illustrated in Fig. 3, which shows the measured γ for the circular polarization channels. A striking polarization dependence is apparent for circularly polarized light in both limits of small and large scattering particles. For small scattering particles, the helicity is flipped by the nondiffusive paths and $\gamma_- < \gamma_+$. For large particles, where forward scattering dominates, the helicity is preserved over a longer length scale than l^*, and this polarization memory results in $\gamma_- > \gamma_+$. This trend is correctly predicted by the values of γ calculated from Eq. (2) using Mie theory, as shown by the solid lines in Fig. 3. The oscillations reflect the resonances characteristic of Mie theory, and would be smeared out by any polydispersity in the scattering particles. The fitted values of n', however, are substantially less than calculated from Mie theory, as shown in the inset of Fig. 2. Nevertheless, they are still larger than n_0, reflecting the large degree of polarization memory. The discrepancy between the data and the Mie theory predictions may be due in part to the effects of particle concentration, and the resulting structure factor, which tends to reduce the forward scattering. This will in turn increase the average angle of scattering
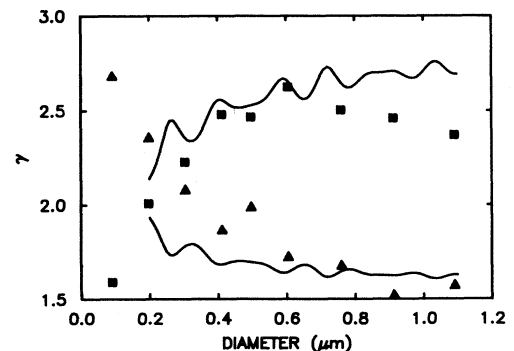

FIG. 3. Measured initial slopes γ for the circular polarization channels as a function of particle size: γ_+ (▲); γ_- (■). Theoretical curves for $\gamma_\pm$ obtained from Eq. (2) using Mie theory (solid lines).

from the individual particles, leading to a less pronounced polarization memory. Consistent with this, increasing ϕ to 0.05 further reduces the observed polarization memory.

A full description of the multiple scattering of light in random media requires a detailed knowledge of the nature of short scattering paths, particularly for backscattering, where the characteristic path length is of order l^*. These nondiffusive paths are responsible for the striking memory of the incident circular polarization. By contrast, linearly polarized light loses its polarization memory as the parti-

cle radius increases, independent of particle concentration, with $\gamma_\parallel$ and $\gamma_\perp$ monotonically approaching the asymptotic value of 2.05 as shown in the inset of Fig. 1. This behavior can be exploited to independently determine τ_0, by measuring the autocorrelation function for both linear polarization channels. This makes particle sizing possible using diffusing-wave spectroscopy,[7] and demonstrates yet another way in which multiple dynamic light scattering can provide useful information about dense media.

[1]M. P. van Albada and A. Lagendijk, Phys. Rev. Lett. 55, 2692 (1985).

[2]P. E. Wolf and G. Maret, Phys. Rev. Lett. 55, 2696 (1985); E. Akkermans, P. E. Wolf, and R. Maynard, Phys. Rev. Lett. 56, 1471 (1986).

[3]S. Etemad, R. Thomson, and M. J. Andrejco, Phys. Rev. Lett. 57, 575 (1986); S. Etemad, R. Thompson, M. J. Andrejco, S. John, and F. MacKintosh, ibid. 59, 1420 (1987).

[4]M. J. Stephen and G. Cwilich, Phys. Rev. B 34, 7564 (1986).

[5]G. H. Watson, P. A. Fleury, and S. L. McCall, Phys. Rev. Lett. 58, 945 (1987).

[6]G. Maret and P. E. Wolf, Z. Phys. B 65, 409 (1987).

[7]D. J. Pine, D. A. Weitz, P. M. Chaikin, and E. Herbolzheimer, Phys. Rev. Lett. 60, 1134 (1988).

[8]F. C. MacKintosh and Sajeev John, Phys. Rev. B 40, 2383 (1989).

[9]M. Rosenbluh, M. Hoshen, I. Freund, and M. Kaveh, Phys. Rev. Lett. 58, 2754 (1987).

[10]G. K. Batchelor, J. Fluid Mech. 74, 1 (1976).

[11]M. J. Stephen, Phys. Rev. B 37, 1 (1988).

[12]M. Kerker, The Scattering of Light (Academic, New York, 1969).